

Synthesis and characterization of spin frustrated Fe doped LiCrO₂

A thesis submitted in partial fulfillment for award of degree in

Master in science

In

Physics

Ms. Aakanksha Sahu

Roll No-412ph2111

Academic year: 2012-2014

Under the guidance of

Dr. Anil K. Singh

Department of Physics and Astronomy



National Institute of Technology,

Rourkela-769008, Odisha, India .

DECLARATION

I hereby declare that the work carried out me at Department of Physics, National Institute of Technology, Rourkela. I further declare that to best of my knowledge the carried out experimental work has not formed the basis for the award of any degree, diploma, or similar title of any university or institution.

Date:

Aakanksha Sahu

Place:

Roll no:- 412ph2111

Department of Physics and Astronomy

National Institute of Technology

Rourkela-769008

ACKNOWLEDGEMENT

First of all I would like to thank the Almighty who enabled me to write this acknowledgement. I would like to express my sincere gratitude to my advisor, Dr. A. K. Singh for giving me the opportunity to work on the exciting research area of condensed matter physics. I deeply appreciate all the time and effort he spent discussing my projects and advising me every now and then. Without his guidance I would have never reached to the completion.

I would also like to thank all other faculty members in the Department of Physics & Astronomy, NIT Rourkela. Specially I would like to thank Professor E. V. Sampathkmaran, Tata Institute of Fundamental Research (TIFR), Mumbai for magnetization measurement. Also, I owe my sincere thanks to the lab members Mr. Soumya Ranjan Mohapatra and Mr. Binayak Sahu of Department of Physics for their guidance. Lastly, I would like to express my heartfelt thanks to my beloved parents for their blessing and my friends for their kind help and wishes for the successful completion of this project.



**Department of Physics and Astronomy,
National Institute of Technology Rourkela
Rourkela-769008, Odisha, India**

CERTIFICATE

This is to certify that the thesis entitled “*Synthesis and Characterization of spin frustrated Fe doped LiCrO_2* ” being submitted by *Ms. AAKANKSHA SAHU* in partial fulfilment of the requirements for the award of the degree of *Masters of Science in Physics* at National Institute of Technology, Rourkela is an authentic experimental work carried out by her under our supervision. To the best of our knowledge, the experimental matter embodied in the thesis has not been submitted to any other University/Institute for the award of any degree or diploma.

Date:

Dr. Anil K. Singh

Abstract

LiCrO₂ and Fe doped LiCrO₂ are prepared by solid state reaction method using LiCO₃, Cr₂O₃, and Fe₂O₃. From XRD data analysis we could confirm the phase purity of all the samples; LiCrO₂, LiCr_{0.98}Fe_{0.02}O₂, and LiCr_{0.95}Fe_{0.05}O₂. All the three samples show dispersion in dielectric constant (ϵ_r) and dielectric loss factor ($\tan \delta$) values. The dielectric constant as a function of frequency at different bias voltage has also been studied. Magnetization measurement for LiCrO₂ using a SQUID magnetometer in a constant magnetic field of 100 Oe under zero field cooled and field cooled condition show the antiferromagnetic transition temperature, $T_N \sim 64$ K. The UV visible plot reveals the slightly increase in band gap due to doping.

CONTENTS

1. INTRODUCTION	Page no
1.1 Magnetism	6
1.2. Ferroelectric material	7
1.3. Ferromagnetic material	8
1.4. Ferro elastic material	8
2. SPIN FRUSTRATION	9
3. MULTIFERROIC	
3.1. Classification	9
3.2. Magneto electric coupling	10
4. APPLICATION	11
5. MOTIVATION	12
6. CRYSTAL STRUCTURE	12
7. SAMPLE PREPARATION	13
8. CHARACTERISATION TECHNIQUES	
8.1. X-ray diffraction	15
8.2. Impedance spectroscopy	16
8.3. FESEM and EDAX	17
8.4. UV visible	18
8.5. SQUID measurement	19
9. RESULTS AND DISCUSSION	
9.1. XRD	20
9.2. FESEM	21
9.3. UV visible	22
9.4. Impedance spectroscopy	23
9.5. SQUID data of LiCrO_2	24
10. CONCLUSION	25
12. FUTURE WORK	25
11. REFERENCES	26

1. INTRODUCTION

Magnetic materials play a very important role in modern life as we know that vast numbers of devices are employed in electromagnetic industry. Before the confinement of quantum mechanics a logical classification of magnetic materials was based up on the response of every material to the magnetic field [1]. In general, it is classified into three categories. They are as follows:

1.1 TYPES OF MAGNETISM

1.1.1 DIAMAGNETISM

Material having no net magnetic moments is called diamagnetic having negative susceptibility. It is the weak form of magnetism. It is induced by a change in orbital motion of electron due to an applied magnetic field. Most of the superconductors shows diamagnetism.

Example- Copper, Gold, Bismuth, Water.

1.1.2 PARAMAGNETISM

Substance which are weakly attracted by magnetic field having net magnetic moments, positive susceptibility, obey Curie's law in which susceptibility is inversely proportional to temperature ($\chi = C/T$) are known as paramagnetic materials. Magnetic permeability is greater than μ_0 . In this kind of materials, magnetic moments are randomly aligned but when magnetic field is applied some of the moments align along the field direction. Paramagnetic materials are used to produce very low temperature by adiabatic demagnetization.

Example- Lithium, Cesium, Tantalum, Sodium.

1.1.3 FERROMAGNETISM

Ferromagnetic materials are strongly attracted by magnetic field. Due to having unpaired electron net magnetic moment exists, shows positive susceptibility, obeys Curie Weiss law ($\chi = C/(T-T_C)$). Temperature at which the exchange energy is greater than the thermal energy and ferromagnetism occurs at that temperature is called Curie temperature (T_C). Exchange energy is minimized when all electrons have same spin.

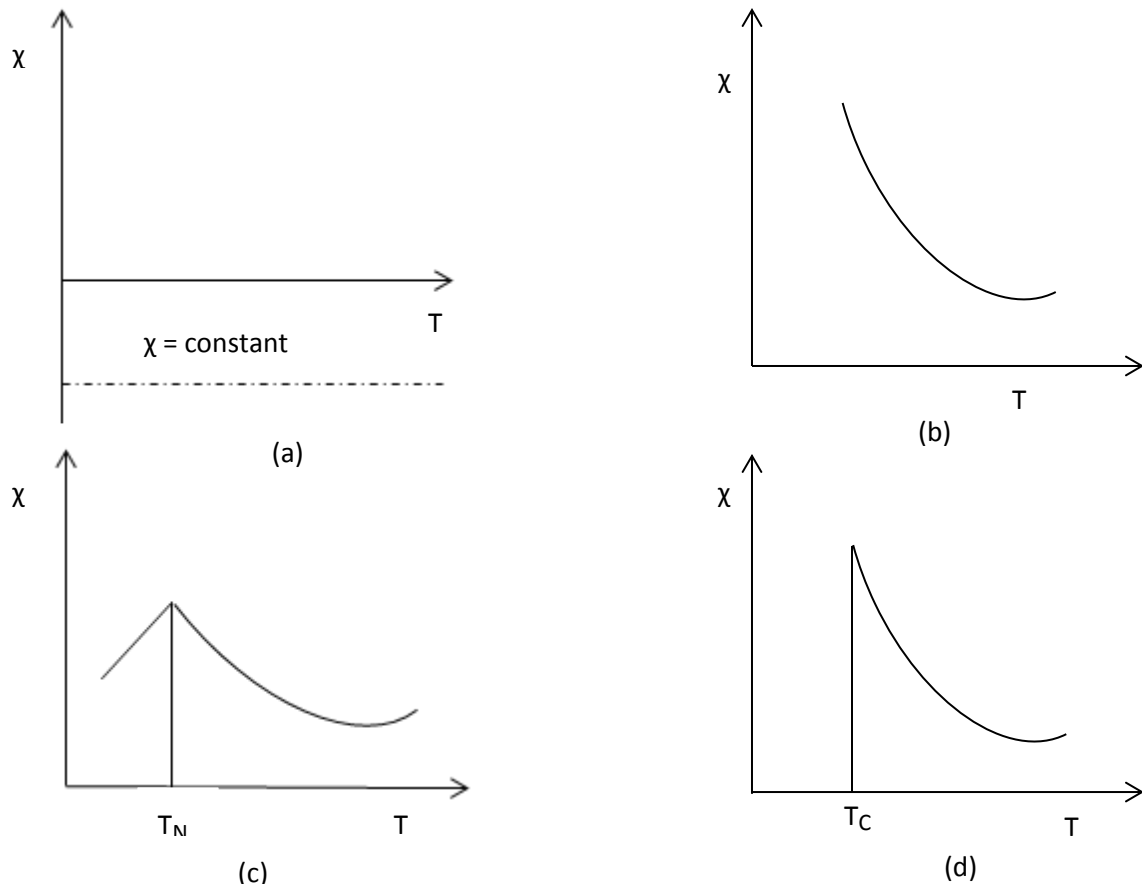


Fig 1.1: Susceptibility versus Temperature graph of (a) diamagnetism (b) para magnetism (c) Ferromagnetism (d) anti ferromagnetism

Now we shall discuss about ferroics. There are three types of ferroics.

1.2 FERROELECTRIC MATERIALS

Ferroelectric materials show spontaneous polarization even in the absence of an electric field. Ions in absence of the field, the positive and negative center do not coincide as a result it creates a dipole moment. Due to the variation of polarization with electric field, it creates a closed loop called the hysteresis loop. The ferroelectric material changes to para electric material after certain temperature T_c , i.e. transition temperature or Curie temperature. These types of crystals are classified in 2 groups: (a) Order-disorder group where the ferroelectric transition

associates with individual ordering of ions. Example of this group is potassium dihydrogen phosphate (b) Displacive group where the ferroelectric transition associates with the displacement of a whole sublattice of ion of one type. The example of displacive group is perovskite and ilmenite structure. And the examples of ferroelectric crystals are barium titanate, Rochelle salt.

1.3 FERROMAGNETIC MATERIALS

Ferromagnetic materials possess spontaneous magnetization, i.e., magnetization exists even in the absence of magnetic field. Large magnetization can be acquired by the material in presence of even a weak external magnetic field. It also possesses a large value of susceptibility but varies with field strength. This variation of magnetization with field strength creates hysteresis curve. The example of these materials Fe, Ni, Co, Gd, Dy and some alloy like MnBi, MnAs, CrO₂.

1.4 FERROELASTIC MATERIALS

Ferroelastic materials possess spontaneous deformation and can be switched hysteretically by an applied stress. Example- Nickel, Titanium.

2. SPIN FRUSTRATION

Spin frustration is also known as geometrical frustration, which is an important feature in magnetism and deals with the topological arrangement of spin. Related features occur in magnets with competing interaction, where both ferro as well as antiferromagnetic coupling between spins or magnetic moments are present depending on separation distance of the spins. In triangular arrangement, ions reside on the corner of the triangle with antiferromagnetic interaction between them and the energy is minimized when the spins are aligned opposite to its neighbors. Once the first two spins are aligned antiparallel, the third one is frustrated because its two possible orientations, either up or down, give the same energy. Similarly, geometric frustration can also be observed in tetrahedral lattice, kagome lattice, pyrochlore lattice etc.

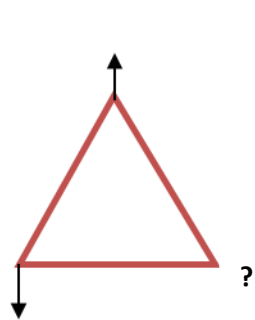


Fig1.2: Antiferromagnetically interacting Spins in triangular arrangement.

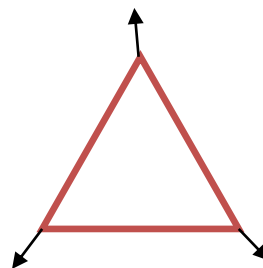


Fig1.3: Spin along easy axis of triangular lattice.

3. MULTIFERROICS

Single phase material which simultaneously possess two or more primary ferroic properties [2] are known as multiferroics. Boracites were probably the first known multiferroics. At first in BiFeO_3 , discovery of a new class of multiferroics shows a large magneto electric effect. A large magnetoelectric effect (a sudden change of electric polarization by the application of magnetic fields) has been observed at the inception field in BiFeO_3 . It was established recently in a class of materials known as ‘frustrated magnets’. There is Perovskites RMnO_3 , RMn_2O_5 (R: rare earths), $\text{Ni}_3\text{V}_2\text{O}_8$, CuFeO_2 , Spinel CoCr_2O_4 , MnWO_4 .

3.1 CLASSIFICATION OF MULTIFERROICS

The magnetism in materials arises due to presence of localized electrons, mostly partially filled d or f shells of transition metals or rare earth ions. But there are several different microscopic sources of ferroelectricity [3] and accordingly we can categorize multiferroics in two classes:

- 1) Type-I multiferroics
- 2) Type-II multiferroics

1) Type-I: In Type-I multiferroics, the cause of ferroelectricity and magnetism are from different sources. In this class of materials, the ferroelectricity typically appears at higher temperatures than magnetism and spontaneous polarisation \mathbf{P} is often large (of the order $10\text{-}100 \mu\text{C}/\text{cm}^2$). Due to this fact, the magnetism and ferroelectricity are independent of each other causing weak coupling between them. e.g. BiFeO_3 , YMnO_3 , LuFe_2O_4 etc.

2) Type-II: In Type-II multiferroics, magnetism causes ferroelectricity implying a strong coupling between the two. In this class of materials, the value of ferroelectric polarization is usually much smaller ($\sim 10^{-2} \mu\text{C}/\text{cm}^2$) and appear at very low temperature (below liquid N_2 temperature) e.g. TbMnO_3 , TbMn_2O_5 , $\text{Ni}_3\text{V}_2\text{O}_8$ etc.

3.2 MAGNETOELECTRIC COUPLING (ME Coupling)

Magnetoelectric coupling has the potential to influence the magnetic state of matter through the application of electric field. In the 1st single phase multiferroics combine both electric and magnetic dipole moments in the same phase but only display low ordering temperature. In 2nd ferroelectric and ferromagnetic phases can be brought in to close contact so that electric and magnetic dipoles coupled via the interface. In both the approaches, the polarization can be a free electron charge near the surface. This phenomenon has been observed in insulating material such as complex multiferroic oxides but not observed in bulk metallic system because applied electric field is screened by a free electron charge near the surface.

The magneto electric effect in a single-phase crystal is described in Landau theory, where free energy is a function of electric field and magnetic field. It may be represented as an infinite homogeneous and stress-free medium by F under the Einstein summation convention in S.I unit as:

$$-F(E, H) = \frac{1}{2} E_i E_j \epsilon_0 \epsilon_{ij} + \frac{1}{2} H_i H_j \mu_0 \mu_{ij} + E_i H_j \alpha_{ij} + \frac{1}{2} E_i H_j H_k \beta_{ijk} + \frac{1}{2} H_i E_j E_k \gamma_{ijk} + \dots$$

Where, ϵ_0 = Permittivity of free space

μ_0 = Permeability of free space

ϵ_{ij} = Second rank tensor

μ_{ij} = Relative permeability

β_{ijk} = Third rank tensor

The magneto electric (ME) effect is the phenomenon of inducing magnetic (electric) polarization by applying an external electric (magnetic) field. The effects can be linear or non-linear with

respect to the external fields. In general, this effect depends on temperature. The effect can be expressed in the following form.

$$\vec{P}_i = \alpha_{ij} H_j + \frac{1}{2} \beta_{ijk} H_j H_k + \dots$$

$$\mu_0 \vec{M}_i = \alpha_{ij} E_j + \frac{1}{2} \gamma_{ijk} E_j E_k + \dots$$

4. APPLICATION

Multiferroics have tremendous application in areas as diverse as data storage, sensing, actuation and spintronics where electric field control of magnetic spin would consume significantly less power than magnetic field control, which requires electric current to generate magnetic fields [4, 5, & 6]. Magnetic field sensor is easier to measure small voltage at zero applied current than small magnetization or small charges in resistivity [7]. Multistage memory elements information are saved in both ferromagnetically and ferroelectric polarization. There is a big hand of magnetoelectric material to improve behind magnetic field sensor.

5. MOTIVATION

In LiCrO₂, lithium has very high storage capacities and chromium oxides have been studied as potential cathode material for rechargeable batteries due to the three electron transfer nature [8]. It is having triangular lattice antiferromagnetic structure, which is the simplest structure among the other spin frustration structure. Its transition temperature T_N = 62 K, which is below the liquid nitrogen temperature. By doping we want to increase the transition temperature to study the magnetoelectric coupling very near to room temperature.

6. STRUCTURE OF LiCrO₂

The element is similar to other ACrO₂ (A = Cu, Ag, Li, Na) having triangular lattice antiferromagnetic where CuCrO₂ and AgCrO₂ have delafossite structure. Each element forms the triangular lattice and stacks along the c-axis. LiCrO₂ and NaCrO₂ crystal are rocksalt structure. Both belongs to same space group $R\bar{3}m$ [9]. From powder diffraction data LiCrO₂ are non-equal two modulations Q= (1/3, 1/3, 1), l=0 and l=1/2. This implies either the magnetic ordering of

LiCrO_2 consist of two domains with $l=0$, $l=1/2$ or that a multi Q structure is established [10]. This rocksalt structure has lattice parameter of $a = 2.8991 \text{ \AA}$, $c = 14.454 \text{ \AA}$.

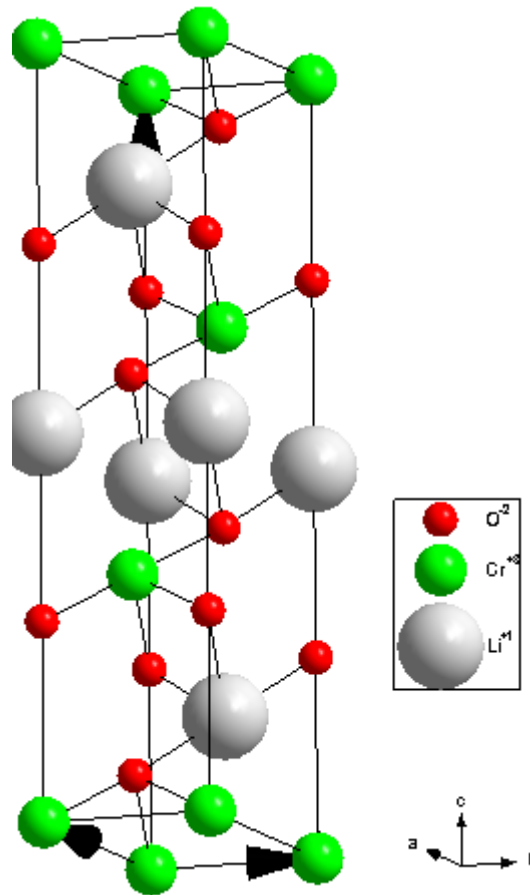
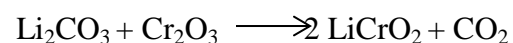


Fig-1.4 Crystal structure of LiCrO_2

7. SAMPLE PREPARATION

The powder specimen of LiCrO_2 was prepared by solid state reaction from stoichiometric mixture of Li_2CO_3 and Cr_2O_3 . They were heated at 1100°C for 24h in air.

It follows the reaction:



- **ATOMIC WEIGHT:** Li - 6.94amu, O - 15.99amu, Cr - 51.9961amu, C - 12.011amu.
- **MOLECULAR WEIGHT:**

$$\text{LiCrO}_2 = 6.94 + 51.9961 + 2 \times (15.999) = 90.9341\text{g}$$

$$\text{Li}_2\text{CO}_3 = 2 \times (6.94) + 12.011 + 3 \times (15.999) = 73.888\text{g}$$

$$\frac{1}{2} \text{Li}_2\text{CO}_3 = 36.9444\text{g}$$

$$\text{Cr}_2\text{O}_3 = 2 \times 51.9961 + 3 \times 15.999 = 151.9892\text{g}$$

$$\frac{1}{2} \text{Cr}_2\text{O}_3 = 75.9946\text{g}$$

$$\text{For 2g of LiCrO}_2, \text{required Li}_2\text{CO}_3 \text{ is } = (36.944/90.9341) \times 2 = 0.81254469 \text{ g}$$

$$\text{For 2g of LiCrO}_2, \text{required Cr}_2\text{O}_3 \text{ is } = (75.9946/90.9341) \times 2 = 1.671421\text{g}$$

7.1. SYNTHESIS OF $\text{LiCr}_{0.95}\text{Fe}_{0.05}\text{O}_2$:

2g of $\text{LiCr}_{0.95}\text{Fe}_{0.05}\text{O}_2$ prepared by solid state reaction method with 0.81829g of Li_2CO_3 , 1.5844g of Cr_2O_3 and 0.08761g of Fe_2O_3 .

Followed by the equation-



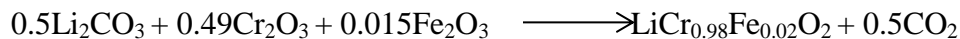
$$\begin{aligned} \text{Molecular weight of Fe}_2\text{O}_3 &= 2 \times 55.845 + 3 \times 15.999 \\ &= 111.69 + 47.997 = 159.687\text{g} \end{aligned}$$

$$\begin{aligned} \text{Molecular weight of LiCr}_{0.95}\text{Fe}_{0.05}\text{O}_2 &= 6.94 + (0.95) \times 51.9961 + (0.05) \times 55.845 + 2 \times 15.999 \\ &= 91.12645\text{g} \end{aligned}$$

7.2. SYNTHESIS OF $\text{LiCr}_{0.98}\text{Fe}_{0.02}\text{O}_2$:

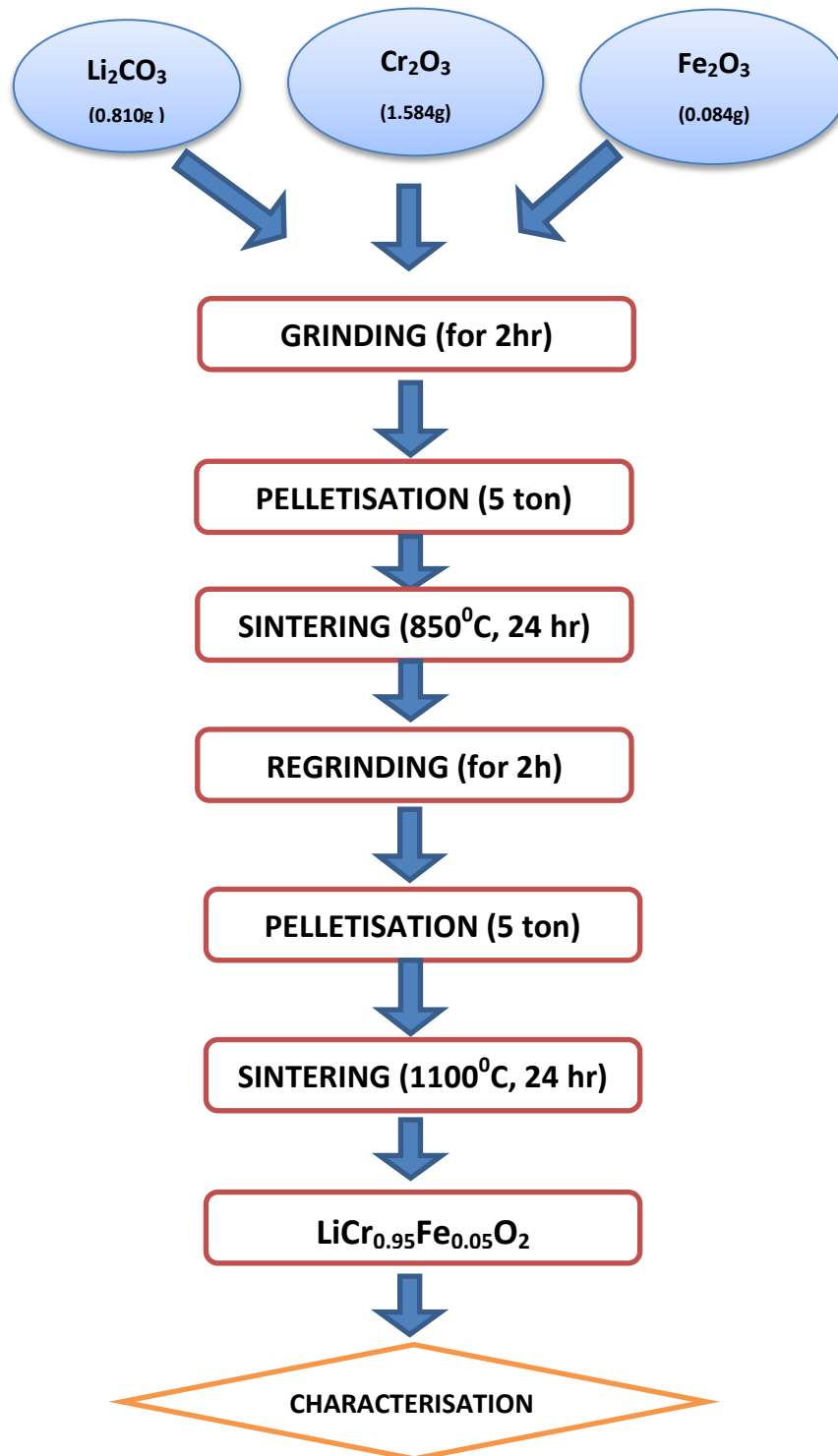
2g of $\text{LiCr}_{0.98}\text{Fe}_{0.02}\text{O}_2$ prepared by solid state reaction method with 0.405928 g of Li_2CO_3 , 1.6366075g of Cr_2O_3 , 0.017548g of Fe_2O_3 .

Followed by the equation-



$$\begin{aligned} \text{Molecular weight of LiCr}_{0.98}\text{Fe}_{0.02}\text{O}_2 &= 6.94 + (0.98) \times 51.9961 + (0.02) \times 55.845 + 2 \times 15.999 \\ &= 91.011078\text{g} \end{aligned}$$

SYNTHESIS PROCEDURE



Similarly, $\text{LiCr}_{0.98}\text{Fe}_{0.02}\text{O}_2$ was also prepared following the above procedure.

PRESSING

At first all the sample are grounded in a mortar pestle for 2h in order to maintain uniform size, then pellets were made by using 10mm diameter of stainless steel die set. We use hydrolic pressed to apply pressure to the powder sample that is of 5 tons. As a result we get a pallets of thickness 1mm.

SINTERING

The pellets were sintered at $850\text{ }^{\circ}\text{C}$ for 2 hours. The ramping rate for cooling and heating was kept at $5\text{ }^{\circ}\text{C}/\text{min}$. Then after first sintering the pellets were broken, again ground for half an hour and again pellets were made. Then it was kept in furnace for second sintering at $1100\text{ }^{\circ}\text{C}$ for 24 hours keeping heating rate the same.

8. CHARACTERISATION TECHNIQUES

8.1 X-ray Diffraction

Bending of light beam from corner of substance is called diffraction. X-ray was produce whenever high speed of electrons collide with a metal target (like Al, Mo, Cu). The interaction of incidence ray produce constructive interference when condition satisfy Bragg's law $2d \sin \theta = n\lambda$ [14] .

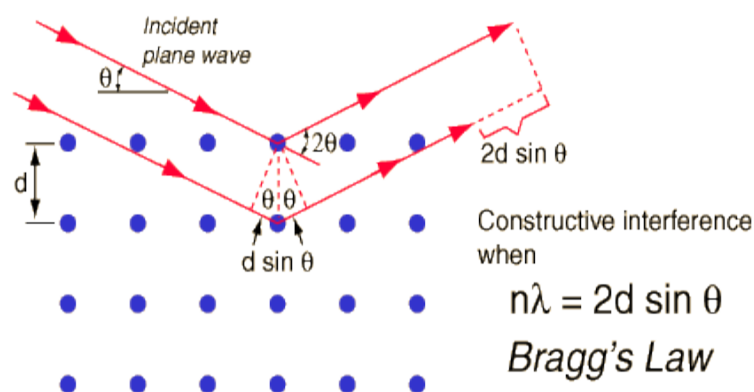


Fig 2.1: Constructive interference represents Bragg's law (Solid state Physics S.O. Pillai, new revised sixth edition)

XRD is a nondestructive technique used to identify crystalline phases and orientation. It is also used to determine structural properties like grain size, strain, lattice parameter, phase composition and to measure thickness of thin film and multi layers.

Different methods of XRD:

<i>Different methods of XRD</i>	λ	Θ
Lau's method	variable	Fixed
Rotating-crystal method	fixed	Variable
Power method	fixed	Variable

8.2. Impedance Spectroscopy:

Dielectric spectroscopy is also known as impedance spectroscopy. It measure the dielectric property of a medium as a function of frequency, based on interaction of an external field with electric dipole moment of the sample. it also measure the impedance which is opposite to the flow of AC in a complex system. Impedance also obey the ohm's law and equals the measure the transfer function $Z(w) = H(w)$. By simple mathematical operation it possible to obtain the magnitude of the measured signal & phase shift between current, voltages. In phasor notation

Real part resistance Real $z = |z| \cos \phi$

Imaginary part Imaginary $z = |z| \sin \phi$

Magnitude of impedance $|z| = \sqrt{(\text{Re } z)^2 + (\text{Im } z)^2}$

Phase shift = $\arctan \left(\frac{\text{Im } z}{\text{Re } z} \right)$

The nature of dielectric material is that dielectric constant decreases with increases in frequency, and constant at higher frequency. The decrease in frequency is due to polarization .This polarization are of three types: 1) Electronic polarization

2) Ionic polarization

3) Dipolar polarization

Variation of polarization can be explained in the basis of relaxation times of above various polarization process. The relaxation time minimum for electronic polarization but maximum for dipolar polarization .

8.3 Field Emission Scanning Electron Microscope (FESEM):

It is an investigative method used in material science, physics and in others branch in order to study the topology, morphology, and composition of the material with much higher resolution .It has a field emission tip for generating charged particle. By maintaining the potential of the electron beam it can be focused to a narrow probing beam of higher energy which results in both improved spatial resolution and minimizes sample charging and damage. When these high energetic electron beam strike on the sample secondary electrons, X-rays and back scattered electrons are ejected from the sample. The detector catches the secondary electron and as a result of which it produce electronic signal. By amplifying and transforming the signal then it changes to scan image .Detecting these electrons with suitable detector we can analyses the sample morphology.

It has many advantages like it produces clear less electrically distorted images with spatial resolution 4-6 times better than that of conventional SEM. In order to study the surface morphology of the present sample NOVA NANO 450 has been used. Due to the non-conducting nature of the sample was been coated with thin layer of gold. It is also used to study the DNA in the cell,synthetic polymer. By the use of EDAX distribution of particle in the sample was known.

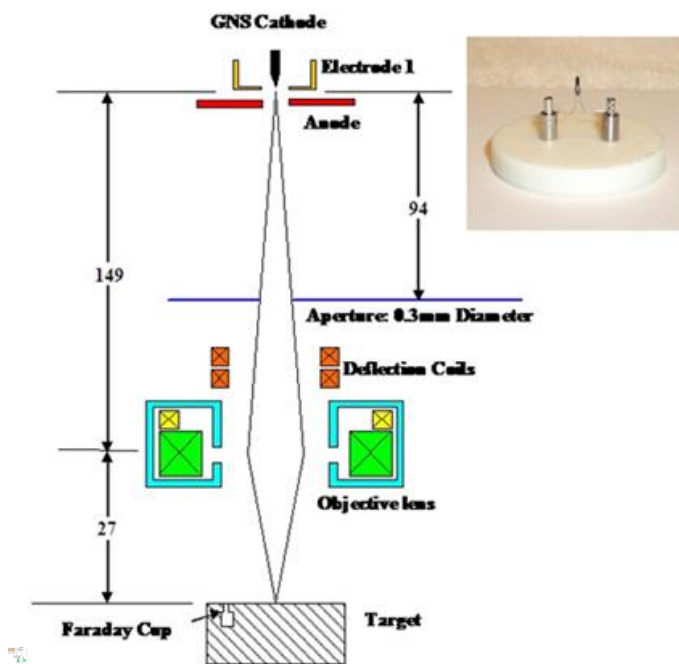


Fig2.2: Schematic diagram of FESEM (www.intechopen.com)

8.4 UV-Vis Spectroscopy:

It generally refers to absorption, reflection spectroscopy in UV-visible spectral region. The absorption or reflection in visible range directly affects the color of the chemicals involved. In the region of electromagnetic spectrum molecules undergoes electronic transition. This technique is while absorbance transition is from the ground state to the excited state. Most of the molecule transition from the π to π^* , it is the best method for determination of impurities in organic molecules. The additional peaks can be observed due to impurities in the standard raw material. We are calculating the band gap by using Tauc equation, which is given as:

$$(\alpha h\nu)^{1/n} = A(h\nu - E_g)$$

Where $n = 1/2$ for direct band gap, $n = 2$ for indirect band gap.

8.5 Superconducting Quantum Interference Device (SQUID)

Superconducting quantum interference device is very sensitive magnetometer to measure the field as low 5×10^{-18} T. There are two types of squid: DC squid, where 2 Josephson junction connected in parallel on a superconducting loop operated in the voltage state with current biased. Second AC/RF squid, where only single electron junction inserted in to a superconducting loop . Squid magnetometer can be performed in two ways. In first measurement temperature dependent magnetic material at constant magnetic field were performed by ZFC. In second measurement temperature dependent magnetization at constant temperature. It uses full application in bio magnetism, scanning squid microscopy, geophysics.

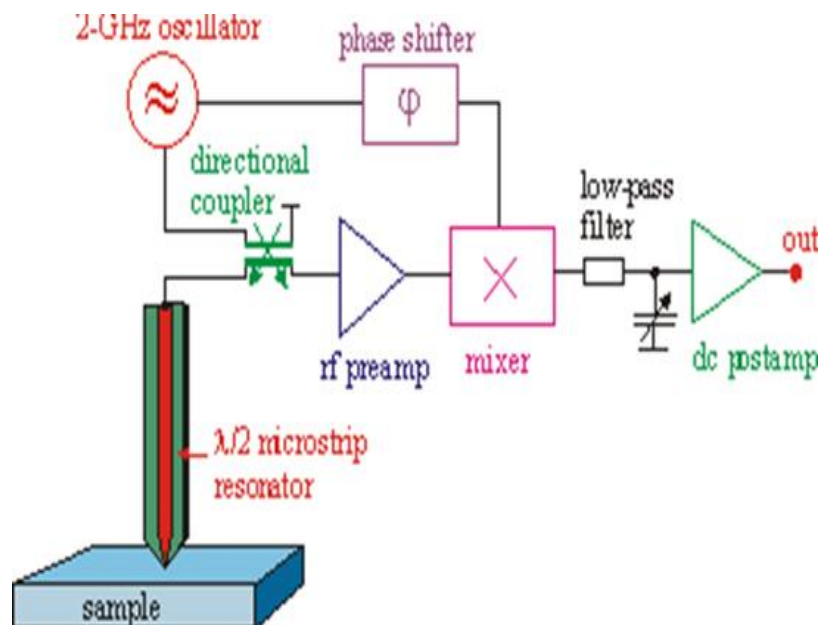


Fig-2.3- Schematic diagram of SQUID (www.ez-squid.de)

9. RESULTS AND DISCUSSION

9.1. X-RAY DIFFRACTION ANALYSIS

In X-ray diffraction, the sample was scanned in a continuous mode from 10° - 80° with a scanning rate 2° per minute. XRD pattern of pure LiCrO_2 is given in figure 3.1. The prominent peaks in the plots are indexed to various [hkl] planes of LiCrO_2 using JCPDFWIN (24-0600).

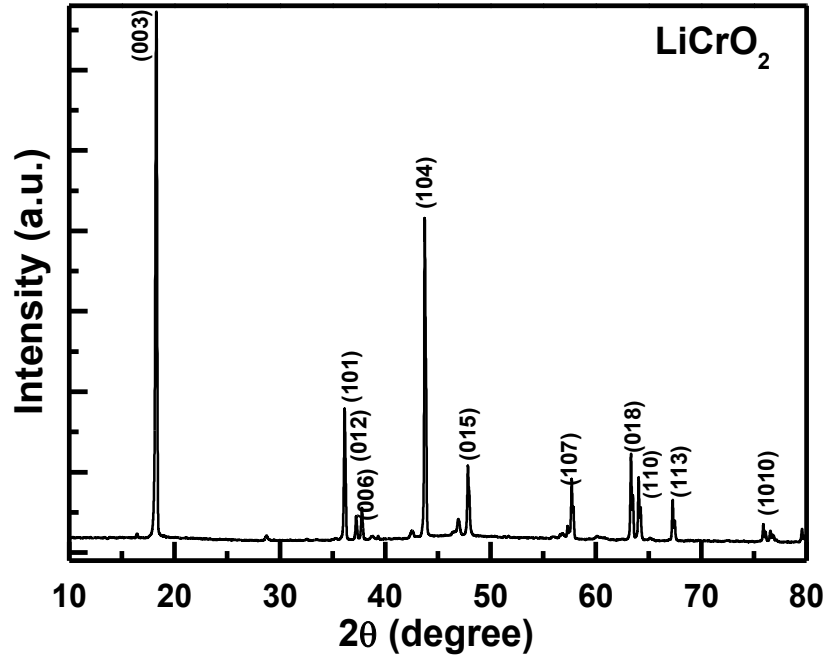


Fig-3.1-X-ray diffraction pattern of LiCrO_2

From the above graph we get no extra impurity peaks by doping and all the peaks are in same phase. By using the formula $d_{hkl} = [4/3\{(h^2+hk+k^2)/a^2+l^2/c^2\}]^{-1/2}$, we have calculated the lattice parameters. Some difference in the lattice parameter are given bellow in table-

Lattice parameter	a (Å)	c (Å)
Pure	14.34	2.89
2% Fe doped	14.49	2.87
5% Fe doped	14.42	2.87

Fig 3.2 shows the comparison between XRD pattern of pure, 2% and 5% Fe doped LiCrO_2 .

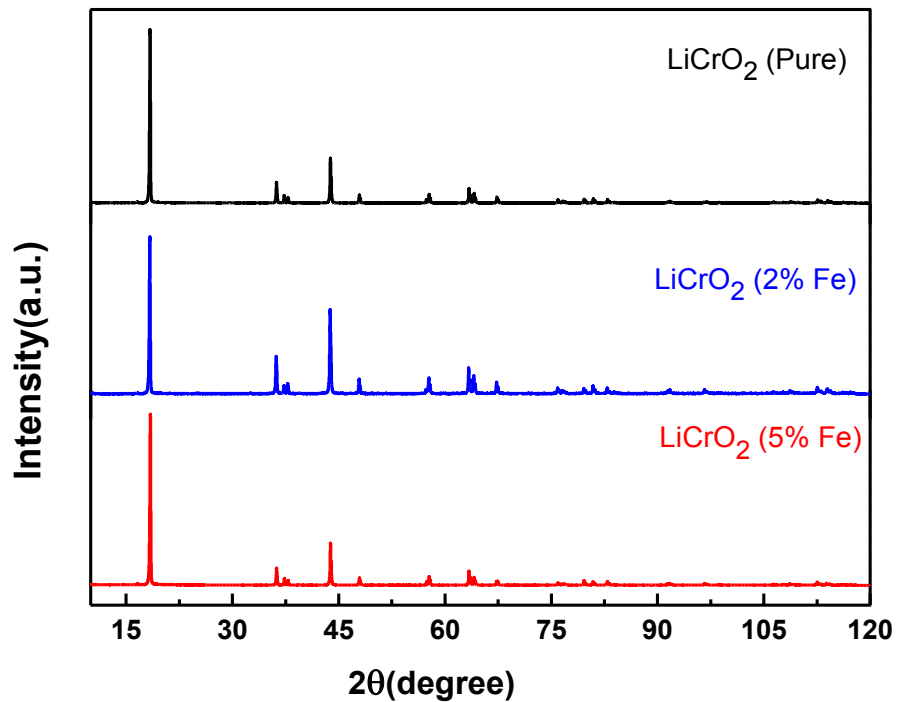


Fig-3.2: XRD plot of Pure, 2% and 5% Fe doped LiCrO_2

9.2. FESEM ANALYSIS

FESEM data reveals that the distribution of grain according to its neighbor atom is not uniform. The percentage of porosity will increase from pure to 2%, 5%. The grain of LiCrO_2 are not well separated but the grains are uniformly distributed.

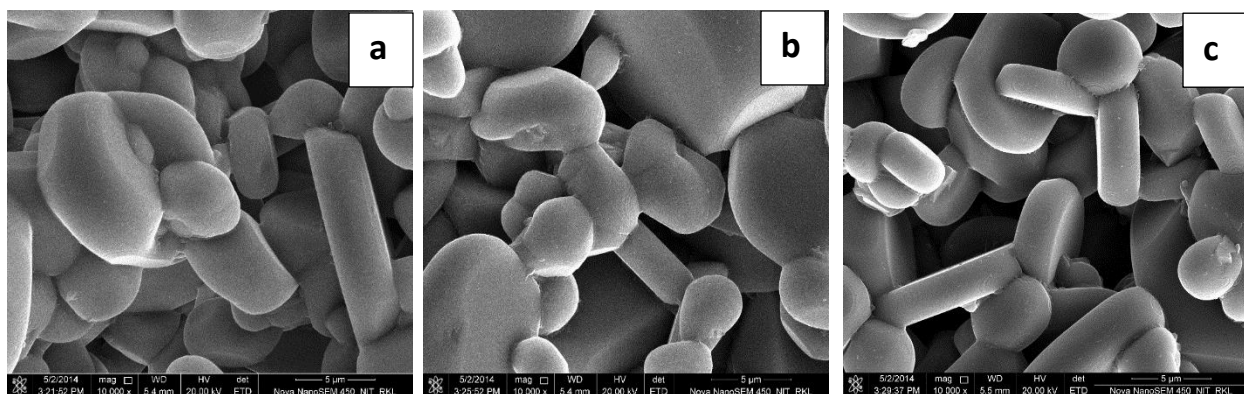


Fig-3.3: FESEM of Pure, 2% and 5% Fe doped LiCrO_2

9.3. UV-VIS ANALYSIS

Graph was plotted between energy and $(\alpha h\nu)^2$. From which we can see where the slope touches the energy curve gives the energy band gap. Thus, from figure 3.4 we determined the band gap for pure LiCrO_2 is 1.74 eV, $\text{LiCr}_{0.98}\text{Fe}_{0.02}\text{O}_2$ is 1.8 eV and $\text{LiCr}_{0.98}\text{Fe}_{0.05}\text{O}_2$ is 1.9 eV.

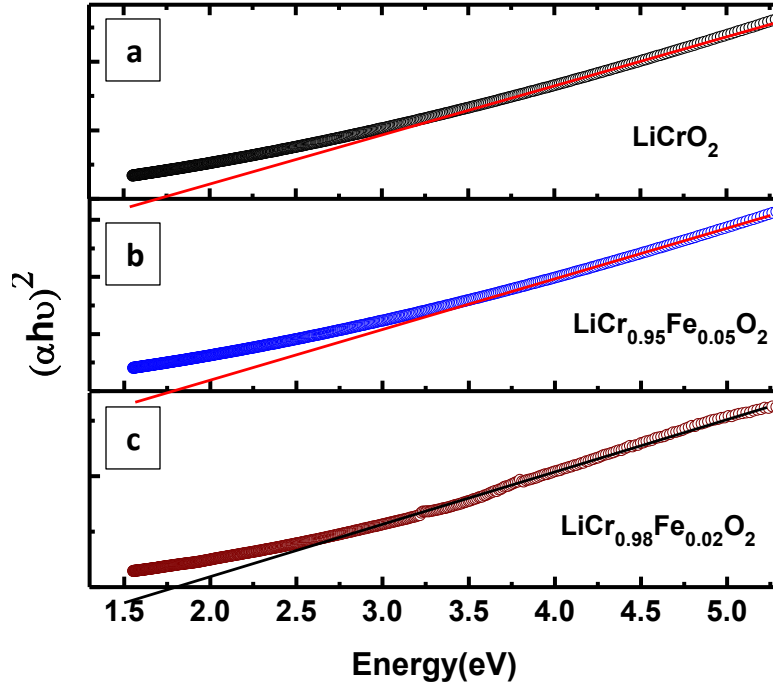


Fig-3.4: Energy band gap of (a) LiCrO_2 , (b) 2% and (c) 5% Fe doped LiCrO_2

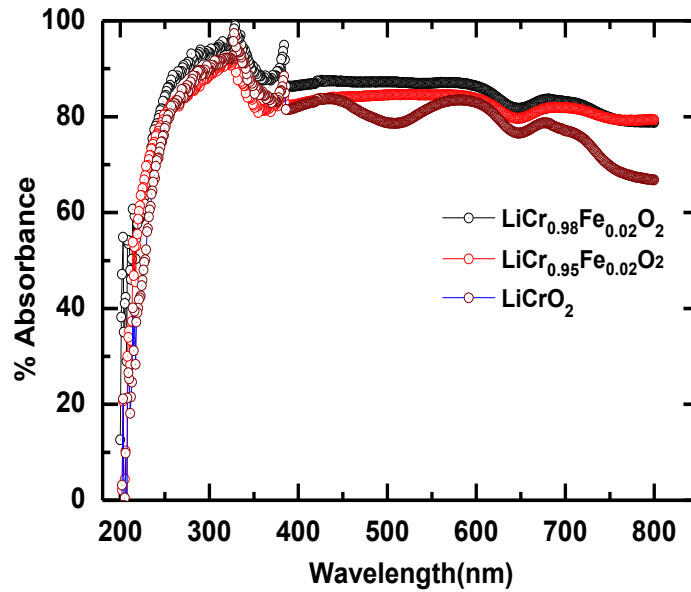


Fig-3.5: Absorption spectra of pure LiCrO_2 , 2% and 5% Fe doped LiCrO_2 .

9.4. DIELECTRIC MEASUREMENT

The dielectric measurement as a function of frequency in the range 100 Hz to 1 MHz is done. Fig 4.1 shows the variation of permittivity as a function of frequency at room temperature for pure and different compositions of LiCrO_2 at a varying bias voltage (1V, 2V, 3V).

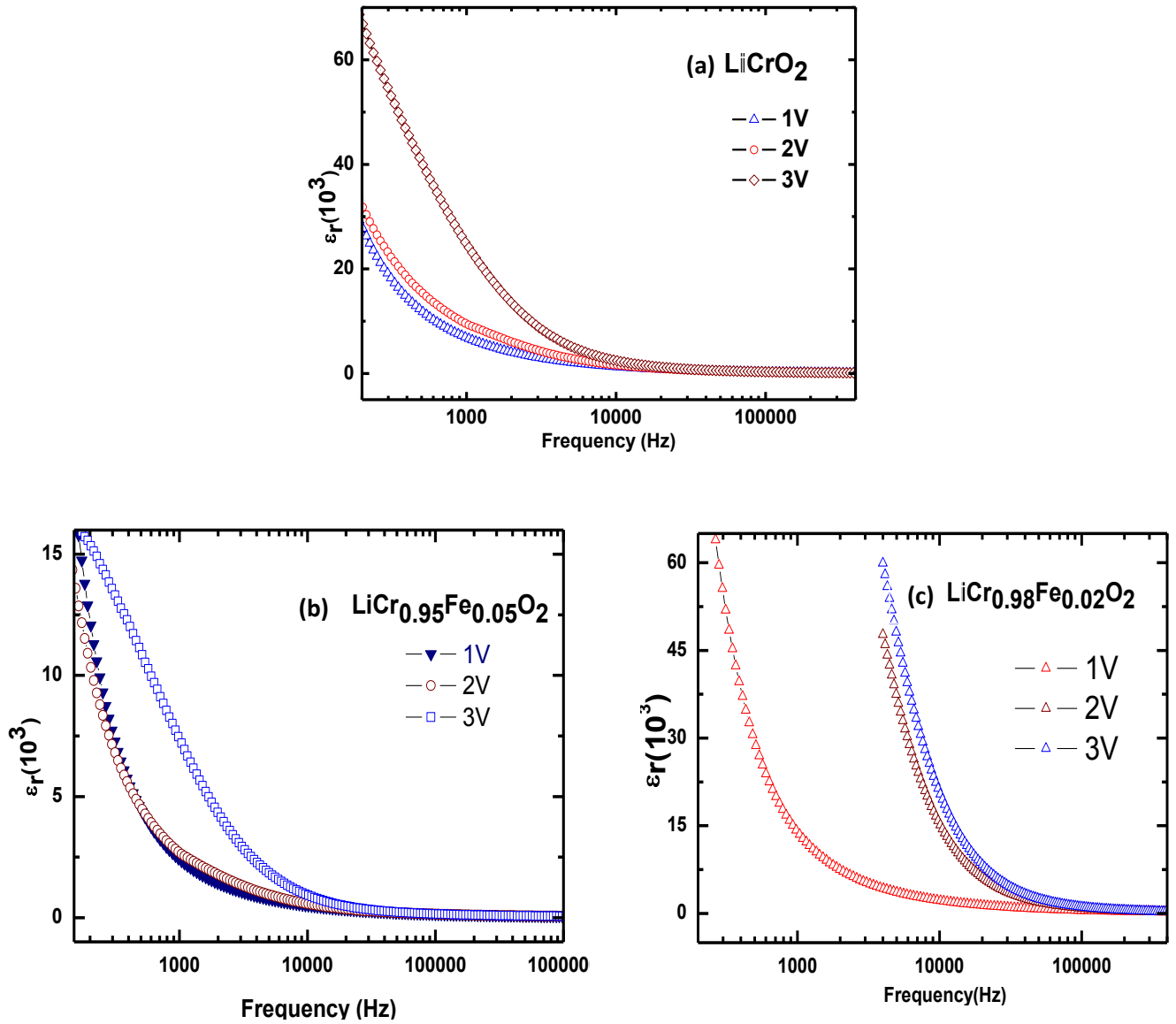


Fig-4.1 Dielectric constant as function of frequency at different bias voltages for (a) LiCrO_2 , (b) 2% and (c) 5% Fe doped LiCrO_2 .

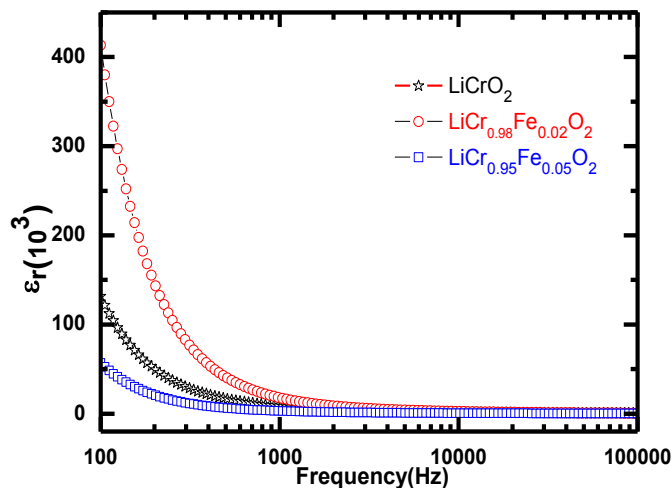


Fig 4.2(a)

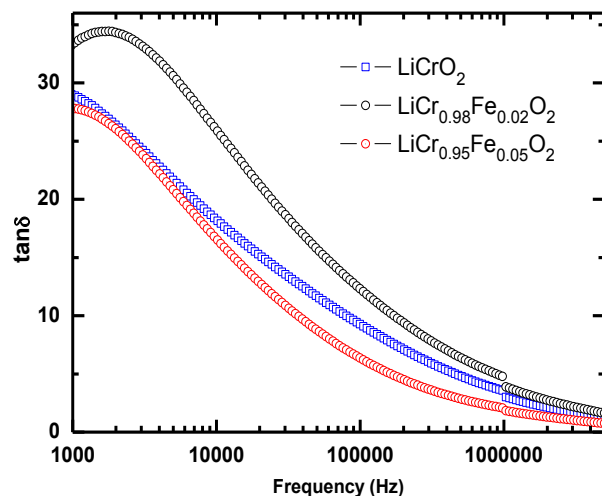


Fig 4.2(b)

Fig-4.2: (a) Permittivity and (b) $\tan\delta$ is plotted as a function of wide range of frequency at room temperature for pure and 2%, 5% Fe doped LiCrO_2 .

Figure 4.2 (a) shows that frequency dependence of these dielectric constant for all three samples at room temperature and figure 4.2 (b) shows the frequency dependence of dielectric loss at room temperature. Dielectric constant decrease with increase in frequency and nearly constant at high frequency. For all three samples obeying the behavior of dielectric materials.

9.5 MAGNETISATION STUDY

Magnetization measurement in a constant magnetic field of 100 Oe under zero field condition and non-zero field condition shows the antiferromagnetic transition temperature, $T_N \sim 64\text{K}$.

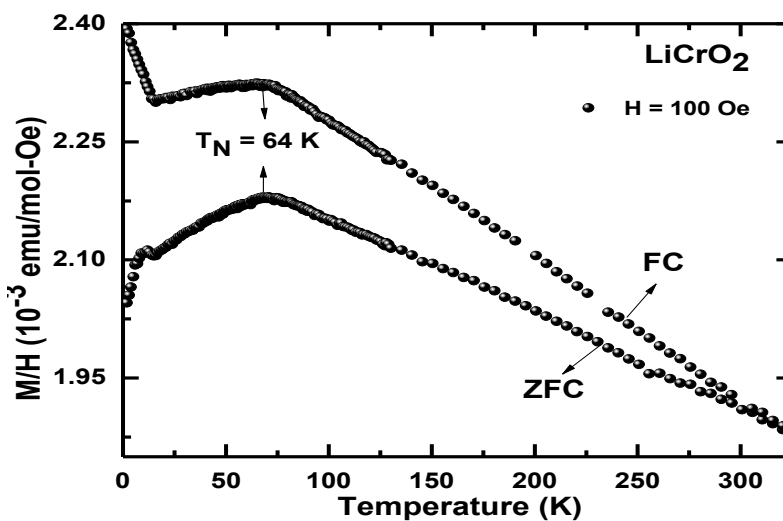


Fig-4.3 Magnetization varying with temperature

10. CONCLUSION

- X-diffraction analysis shows that due to doping (2%, 5%) Fe crystal, structure remains the same as that of the pure LiCrO_2 .
- From FESEM data we confirm that the porosity increases as doping percentage increases.
- The dielectric measurement shows that dielectric constant increases due to 2% doping and decreases due to 5% doping as compared to pure LiCrO_2 .
- UV- Visible study reveals that the band gap gradually increases due to doping. The band gap as calculated are: 1.7 eV (LiCrO_2), 1.8 eV ($\text{LiCr}_{0.98}\text{Fe}_{0.02}\text{O}_2$) and 1.9 eV ($\text{LiCr}_{0.95}\text{Fe}_{0.05}\text{O}_2$).
- Magnetization data at a constant magnetic field of 100 Oe under ZFC and FC shows that the antiferromagnetic transition temperature, $T_N = 62$ K.

11. FUTURE WORK:

1. Dielectric constant as a function of low temperature.
2. Dielectric measurement in the higher temperature regime (300 K-700 K) is not studied.
3. Magnetization measurement of various doped sample.
4. Sample preparation of higher Fe doping and perform similar kind of study.
5. Doping at nonmagnetic site may give better understanding to the system.

11. REFERENCE

- 1) Introduction to Solid State Physics, Charles Kittel, Wiley Student's 7th Edition and solid state physics V. K. Babbar, R.K. Puri.
- 2) D. I. Khomskii, Bull. Am. Phys. Soc. C **21.002** (2001).
- 3) Classifying multiferroics: Mechanisms and effects, D. Khomskii, Phys. **77**, **50937** (2009).
- 4) M. Fiebig, J. Phys. D Appl. Phys. **38**, **R123 73**, **235113**(2006)
- 5) Special issue, J. Phys. Condens. Matter **20**, **434201** (2008).
- 6) R. Ramesh and N. A Spaldin, Nature Mater. **6**, **21** (2007);
- 7) J. Zhai et al., Appl. Phys. Lett. **88**, **062510** (2006).
- 8) G. X. Feng, L. F. Li, J. Y. Liu, N. Liu, H. Li, X. Q. Yang, X. J. Huang, L. Q. Chen, K. W. Nam and W.S. Yoon J.Mater.chem,**19**, **2993** (2009).
- 9) S. Seki, Y.Onose and Y.Tokura Cond-mat. Str-el arXiv:**0801.3151V**(2008)
- 10) H. Kadowaki et al., J. Phys.: Condens. Matter **7**, **6869** (1995)
- 11) Fig-2.1-constructive interference represent BRAGG'S LAW (Introduction to Solid State Physics, Charles Kittel, Wiley Student's 7th Edition)
- 12) Fig2.2-Schematic diagram of FESEM (www.intechopen.com)
- 13) Fig-2.3- Schematic diagram of SQUID (www.ez-squid.de)
- 14) Element of x-ray diffraction by B.D.CULLITY